Royal Norwegian Council for Scientific and Industrial Research

3

ERRORS IN TIME DELAY MEASUREMENTS

by

H. Bungum and E.S. Husebye

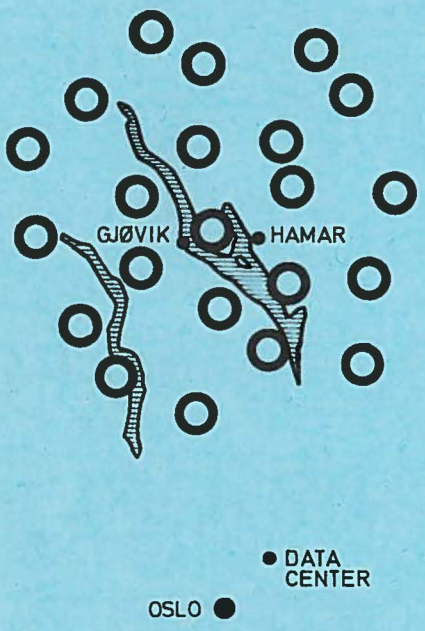

NORWEGIAN SEISMIC ARRAY

NORSAR

P. O. Box 51. 2007 Kjeller – Norway

NTNF/NORSAR
Post Box 51
N-2007 Kjeller
Norway

NORSAR Report No. 3

ERRORS IN TIME DELAY MEASUREMENTS

by

H. Bungum and E.S. Husebye

31 December 1970

The NORSAR research project has been sponsored by the United States of America under the overall direction of the Advanced Research Projects Agency and the technical management of Electronic Systems Division, Air Force Systems Command, through Contract No. F19628-70-C-0283 with the Royal Norwegian Council for Scientific and Industrial Research.

ERRORS IN TIME DELAY MEASUREMENTS

by

H. Bungum and E.S. Husebye

Abstract

Simple delay and sum of sensors in a seismic array is an effective method for noise suppression. However, unless we have precise steering delays, much of the signal energy is lost during the beam forming process too. We have investigated possible error sources in time delay measurements, using a computerized cross-correlation procedure. Parameters perturbed are correlation window length and positioning, signal frequency content and signal to noise ratio (SNR). Our results indicate that relative low frequency waves and using the very first part of the P-signals give the most reliable and stable time delay values. High frequency bandpass filtering improves SNR, but signal correlation and the precision in beam steering corrections decrease. Significant loss of high frequency energy during beam-forming seems to be unavoidable.

1. Introduction

Observations and subsequent analysis of travel times of seismic waves, especially P-waves, play a fundamental role in seismology. Considering a seismic array like NORSAR, we require very high accuracy in the time delays (station corrections) for two reasons. First, the array's event detection capabilities are critically dependent on the quality of the steering delay data used during the beam-forming process. The loss in array gain due to erroneous time delays is frequency dependent and expressible as: (Steinberg, 1965)

$$\text{Loss (in dB)} = 170(\sigma/\tau)^2 \qquad (1)$$

where σ is the standard deviation (STD) in the time delay measurements, and τ is the dominant signal period. Second, seismic array data is extensively used for direct measurements of the $dT/d\Delta$ parameter, which is an efficient tool for detailed investigations of the Earth's structure. In this

case too, precise time delay measurements are required for compensating for the relatively small dimensions of the array (as compared to a continental array).

The purpose of our study is to investigate possible sources of errors in P-wave travel time delay measurements. The method in use (IBM 1967, b) is straightforward - a computerized cross-correlation iteration scheme - but the final result may depend on signal frequency, signal length used and signal to noise ratio (SNR).

2. Methods for measuring travel times

Visual insepction of an ordinary seismograph record gives reliable travel time measurements under favorable conditions. Further improvements are obtainable when a number of recordings from adjacent stations, say, an array, are available using the fact that P-signals exhibit a high degree of similarity even for large station separations (Jansson & Husebye 1968). Working with analog data, the common procedure is a line-up of the traces by a visual comparison of the individual signals. This simple method is very powerful, but time-consuming. When adapted to a computer the signal line-up is performed by cross-correlation calculations.

For a large array like NORSAR (Figure 1), characterized by digital data recording at a sampling rate of 10 Hz, the procedure for measuring time delays is as follows. It should be noted that recently NORSAR sampling rate has been changed to 20 Hz, but data analysis is normally limited to a 10 Hz sampling rate. We start with forming an array beam using a preliminary set of time delays, say the Detection Processor estimate. The single sensor signals are successively cross-correlated with the beam trace. The correlation operation is limited to a time window which positioning depends on either arrival time or maximum energy of the P-wave. From the maximum values of the correlation functions, a new and improved set of time delays is computed, and then a new beam

is formed. The above process is iterated until it converges, i.e., until the adjusted time delays remain unchanged between two consecutive runs. In case of no convergence, the program stops when a specified number of iterations are performed. The final solution is given in fractions of the sampling frequency, after applying a least squares interpolation formula to the last set of cross-correlation functions for precise peak locations. To facilitate visual inspection of the computer solution, a computer plot of beam and sensor traces for each event analyzed (Figure 2) is produced.

3. Data analysis

From the previous section we may conclude that the method for computing time delays is straightforward. However, the implicit definition of the P-signal in such measurements represents an intrinsic problem and subsequently a source of undesired errors. In order to investigate this phenomenon we have analyzed a few events (Table 1) by systematically perturbing the following signal parameters:

1. Magnitude or the related parameter SNR
2. Positioning of the cross-correlation window
3. Length of the cross-correlation window
4. Signal spectra content

We have used a rather comprehensive perturbation procedure as the above parameters are not independent of each other. For example, signal descaling or magnitude variation give different results for signals having different spectral distributions. Anyway, the test procedure in detail is as follows:

1. Signal magnitude simulation is performed by multiplying the signal amplitudes by a constant (K) and then adding the resulting wave to the preceding noise. By setting $K=2^{-n}$, $n=1,2,\ldots$, this corresponds to magnitude decrease in steps of about 0.3 units.

2. Window positioning is either fixed at P-signal onset (standard) or related to maximum signal power measured in a window of specified length.

3. Window length options are 24, 32 (standard value) and 40 dsec.

4. Signal spectral variation is simulated by using recursive third order Butterworth bandpass filters. Four different sets of filters are tested, each set characterized by a fixed bandwidth. Each set contains five filters which are arranged in a comb pattern and comprise a total frequency band of around 0.5-4.0 Hz. The filters are displayed in Figure 3 and filter set C (bandwidth 2.0 Hz) is normally used.

As we are investigating possible errors in computerized time delay measurements, certain criteria are required for judging performance. With performance we mean that set of signal parameters which in average five the most reliable and stable measurements of time delays. The criteria are:

1. Differences between calculated and observed P-wave velocity and azimuth. Observed values are based on a least squares plane wave to fit to the measured time delay values.

2. Standard deviations (STD) of velocity and azimuth estimates, and STD of time residuals, i.e., the difference between observed time delays and those predicted from a least squares plane wave solution.

3. Cross-correlation values and the number of "bad" sensors. "Bad" sensors are those which either are obviously miscorrelated (like being one cycle off), or those which have a waveform too incoherent as compared to the beam.

4. The power loss suffered during the beam-forming process.

None of the above criteria is quite satisfactory, and one of the most complicating factors is that the wavefront, due to structural anomalies, deviates from a plane. However, in general we prefer the estimator (out of the class of all unbiased estimator) which has the minimum variance.

Intuitively we should expect performance in terms of the criteria outlined above to vary smoothly but slowly from bad to good. Due to the dependence of the signal generation on seismic regions, we will be satisfied to specify a signal parameter set to be used routinely in time delay measurements which ensures an overall good performance. We are less interested in parameter specification which gives a mixture of excellent and fair performances for the events analyzed. In any case, the routine analysis has to be followed by a rerun of some of the more complicated events, where some of the parameters are changed.

4. Results

The results of this time delay measurement analysis will be presented according to the set of signal test parameters discussed in the previous sections.

4.1 Signal magnitude

Using the amplitude descaling procedure described above, the signal magnitude becomes critical when reaching a lower threshold value. This limit depends of course on noise level, but also on signal frequency as demonstrated in Figure 4. Although SNR increases with increasing frequency, this gain is partly offset by decreasing signal similarity or coherency. The latter effect is demonstrated in Figure 5. In short, in the frequency range 0.7-3.0 Hz (bandwidth around 1.6-2.0 Hz) reliable time delays are measurable for SNR around 2.0 or larger. A rough estimate of the corresponding magnitude range gives 4.5-5.0. Signal to noise ratio gain by digital filtering of the respective signals amounts to around 12-18 dB or 0.6-0.9 magnitude units. When we have data available from all 6 sensors in the NORSAR subarrays, we will have an additional gain in SNR amounting to around 7-8 dB.

4.2 Window positioning

From the point of view of event detection capability, it may be advantageous to tie the steering delay measurements to the position of maximum amplitudes or power in the P-signal. In

practice, there are several objections to such a procedure. For example, a P-wave consists of a rather pure P-signal (first part) and signal generated noise (latter part) containing relatively high frequencies (Figure 4). The latter, usually denoted the coda, is due to small-scale scattering sources close to the receiver and/or source. The coda sometimes have a purely random nature, causing a large signal suppression during beam-forming. Other times specific scattering sources are detectable as demonstrated by Capon (1969) and Mack (1969). Our results from window positioning reflect this arbitrary behaviour of the later part of the P-signal, and are characterized by relatively small correlation values and significant differences between observed and calculated velocity and azimuth (Table 2). To ensure stable and reliable time delay measurements, we must require that the cross-correlation window is restricted to the first part of the P-signal.

4.3 Signal spectra

Bandpass filtering gives a substantial gain in SNR (Figure 5), and this largely increases the number of events acceptable for analysis. Concerning time delay measurements, the performance here depends on signal coherency as well. This problem has been investigated by prefiltering, using four sets of recursive Butterworth filters (Figure 3) before analysis. Some of the results obtained here are displayed in Figure 6. A brief summary of performance as function of filter setting gives:

Filter sets C and D, which are characterized by large bandwidths (2.0 and 2.4 Hz), have the best performance. Common for all filter sets is that acceptable solutions are obtained when the filter pass band comprises most of the frequency range 1.0-2.4 Hz. However, for narrow band filters a relatively large number of sensors are rejected from analysis due to poor or ambiguous cross-correlation functions. Low frequency filters always give good results for strong events,

but the SNR gain from filtering is then small due to poor noise suppression (Figure 5). In short, a minimum bandwidth of around 1.6 Hz and pass band coverage of the frequency range 0.9-2.5 Hz will ensure in average the most stable and reliable time delay measurements. When using more broad band filters, low energy, high frequency components of the signal are retained in analysis, but this effect seems negligible as demonstrated above.

4.4 Length of cross-correlation window

Tentatively window length values of 24, 32 and 40 dsec have been tested, using filter set C, having a bandwidth of 2.0 Hz. In terms of absolute values of observed velocity and azimuth and the corresponding STD values, measurements as function of window length are not critical. Although differences are small, a window length of 24 dsec gave best results for the events analyzed (Figure 7). We should here like to point out that the sensor traces rejected from analysis, may vary from one case to another, and thus make it sometimes difficult to compare directly the individual results during the perturbation analysis. In addition, the shortest window length gives largest cross-correlation values, and is least troubled with bad sensor traces. On the other hand, a smaller window length requires a better initial steering of the array. A window length of about 28 dsec seems to be the best compromise.

A single analysis requires about 4 min of computer time, and thus somewhat restricts the number of events to be analyzed for extensive test parameter combinations. In our opinion the choice of the proper bandpass filter is the most uncertain factor in time delay measurements, so a further test of this parameter limited to filter set C was conducted. Some of the results obtained here are displayed in Figure 8, and confirm the previous recommendation of a center frequency around 2.0 Hz.

5. Discussion

The two major reasons for performing time delay measurements are to provide steering delays for routine event detection (seismic surveillance) and $dT/d\Delta$ calculations. In the latter case we require beside high precision in the time delay measurements themselves, also a proper array configuration. For example, excluding a few of the C-ring sensors (Figure 1) may alter the observed $dT/d\Delta$ and azimuth values about 0.1 sec/deg and 1° which sometimes exceed the STD of these parameters. As steering delays may be tied to a reference station, array configuration is not that critical in such cases. On the other hand, the full aperture of NORSAR is needed for calibrating the location parameters. Therefore, to ensure a rapid accumulation of steering delays and $dT/d\Delta$ data, the recommended signal parameters for time delay measurements should be used. These are: correlation window coverage of the very first part of the signal, window length around 28 dsec, center frequency of filter pass band around 2.0 Hz and a bandwidth of around 2.0 Hz. For poor events, i.e., events having poor SNR and located in regions of low seismic activity, the time delay measurements will be more successful using a center frequency around 2.5 Hz. It should be noted that experience gained from time delay analysis of around 250 NORSAR events is in good agreement with the above recommendations.

Finally, we should like to discuss some aspects of the consequences of the recommended parameter set for the time delay measurements. First of all, the steering delays are tied to a specific frequency band of the signals which not necessarily give the same time delays for another band as demonstrated above. This means that possible biased errors are introduced in analysis of beam traces due to frequency dependent signal suppression as a function of faulty steering. In addition, from an event detection point of view we may also argue that the noise suppression due to high frequency bandpass filtering can be larger than the signal losses on the beam level caused by erroneous steering delays.

However, despite the above objections, we still will recommend the above parameter set for time delay measurements as this seems to be the only way to ensure a rapid accumulation of a stable and reliable steering delay library for the NORSAR array. In short, the P-wave coda is too complex and incoherent across the array to warrant time delay measurements tied to this part of the signals.

Acknowledgement

Valuable advice and discussions with J. Felix, IBM, Federal Systems Division, USA, are greatly appreciated.

References

Capon, J.; Continental Aperture Seismic Arrays, Semiannual Technical Summary, MIT Lincoln Lab, June 1969.

IBM (1967,a); LASA Signal Processing, Simulation, and Communications Study, IBM Final Report, ESD-TR-66-635, Gaithersburg, Maryland, USA, Mar 1967.

IBM (1967,b); LASA Experimental Signal Processing System, IBM Third Quarterly Technical Rep., ESD-TR-68-149, Gaithersburg Maryland, USA, AUG 1967.

Jansson, B., and E.S. Husebye; Application of Array Data Technique to a Network of Ordinary Seismograph Stations, Pure and Applied Geophysics, Vol 63, pp 83-104, 1966/I.

Mack, H.; Nature of Short-Period P-Wave Signal Variations at LASA, J. Geophys. Res., 74, pp 3161-3170, 1969.

Steinberg, B.; Large Aperture Teleseismic Array Theory, ARPA Report of First LASA Systems Evaluation Conference, 1965.

Table Captions

Table 1: Data for seismic events used in this paper.

Table 2: STD of time delays, $dT/d\Delta$ and azimuth as a function of different window positions.

Figure Captions

Figure 1: The NORSAR array configuration. Sensors in subarrays 01A, 03B, 04B and 06B are not included in the Plan D configuration.

Figure 2: Sensor and beam signal line-up as part of the computerized time delay measurement. The vertical line marks the center of the cross-correlation windows. The signals are scaled individually and in nanometer per inch (NM/IN).

Figure 3: The four filter sets A,B,C,D used in analysis. They are third order recursive Butterworth bandpass filters (IBM, 1967, a).

Figure 4: Event 1 beams as a function of magnitude and different passband filters. The vertical bars mark the correlation window (32 dsec) which is tied to maximum energy of the beam signal. The number to the left gives the Butterworth filter passbands.

Figure 5: Relative gain in SNR due to filtering, using filter set C. Solid and broken lines refer to beams and single sensor traces respectively.

Figure 6: Sections a,b,c,d give respectively no. of sensors rejected from analysis, STD of time residuals, observed $dT/d\Delta$ and azimuth values for events 12 and 13. In the latter case the results are in brackets. All filter sets have been used.

Figure 7: No. of sensors rejected from analysis (in brackets) and STD of time residuals for different lengths of the correlation window. Events 11,12,13 and filter set C have been used.

Figure 8: STD of time residuals for filter set C. Event numbers are in brackets.

Table 1

Event	Origin Time Date	h m s	Lat.	Long.	Depth	Mag.	Dist.	Azi.	dT/dΔ	Region
1	30 Nov 1969	03.32.57,2	49.9N	79.0E	0	6.0	38.9	76.2	8.30	Kazakh
2	26 Dec 1969	00.18.21,1	55.2N	160.4W	25	5.3	63.9	353.8	6.50	Alaska
3	10 Jan 1970	12.07.08,6	6.8N	126.7E	73	6.1	96.2	64.0	4.55	Philippine Isl.
4	27 Jan 1970	10.49.31,4	34.9N	101.3E	33	5.1	60.3	70.9	6.80	Tsinghai, China
5	27 Jan 1970	11.17.29,4	57.7N	163.6E	41	5.1	59.7	16.5	6.85	Near Kamchatka
6	29 Jan 1970	06.03.21,7	35.9N	140.4E	70	5.1	75.0	40.3	5.75	Near E. Honshu
7	30 Jan 1970	17.10.22,4	43.3N	146.8E	45	4.5	70.0	32.7	6.10	Kurile Islands
8	31 Jan 1970	11.41.53,6	4.1N	96.0E	56	5.3	84.1	92.1	5.00	N. Sumatra
9	2 Feb 1970	17.22.08,0	43.5N	147.5E	33	5.5	70.0	32.1	6.10	Kurile Islands
10	6 Feb 1970	00.11.49,6	54.6N	163.6E	43	5.6	62.7	17.4	6.65	Off E. Kamchatka
11	7 Feb 1970	23.36.53,3	47.3N	154.0E	33	5.0	68.0	26.1	6.25	Kurile Islands
12	10 Feb 1970	10.40.39,0	36.2N	140.0E	67	4.9	74.6	40.5	5.80	Near E. Honshu
13	12 Feb 1970	01.51.51,4	29.4N	81.6E	44	5.4	55.4	90.8	7.20	Nepal

Table 2

Event No.	TIME LAG (DSEC) FROM FIRST ONSET 0	10	20	30	50	Parameters
2	0.991	1.028				STD
	6.50 ± 0.133	6.51 ± 0.130	No solution	No solution	--	dT/dΔ
	355.37 ± 1.27	355.22 ± 1.24				Azi.
3	1.617		1.781	1.622	1.611	STD
	5.28 ± 0.149	No solution	5.15 ± 0.165	5.26 ± 0.165	5.26 ± 0.148	dT/dΔ
	65.55 ± 1.73		58.01 ± 1.95	66.82 ± 1.75	66.78 ± 1.73	Azi.
9	0.860	0.850	0.786			STD
	6.49 ± 0.078	6.51 ± 0.077	6.52 ± 0.071	--	--	dT/dΔ
	31.36 ± 0.92	31.45 ± 0.91	31.76 ± 0.84			Azi

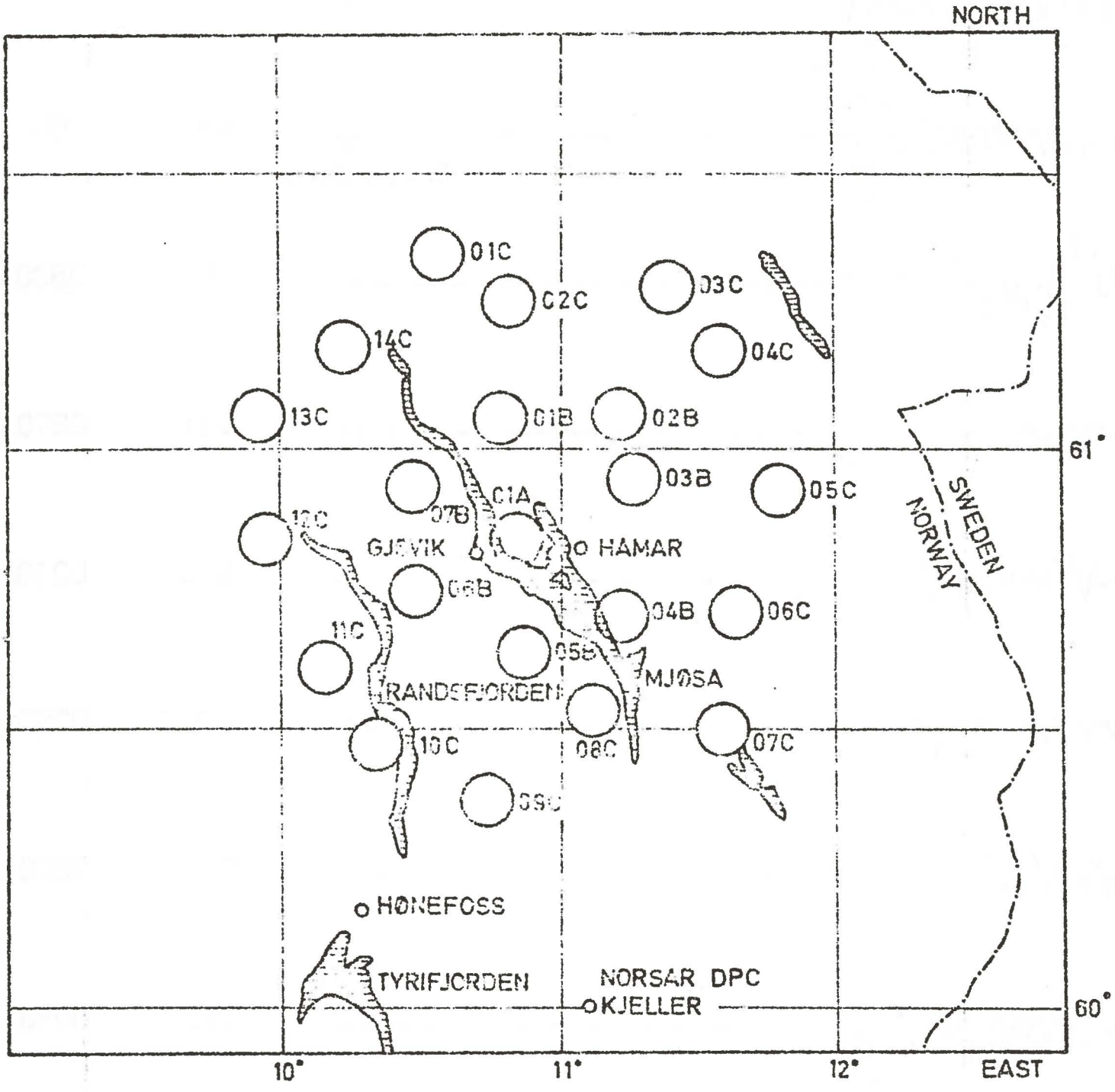
NORTH
01C
02C
03C
14C
04C
13C
01B
02B
03B
05C
07B
01A
12C
GJØVIK
HAMAR
06B
04B
06C
11C
05B
MJØSA
RANDSFJORDEN
10C
08C
07C
09C
HØNEFOSS
TYRIFJORDEN
NORSAR DPC
KJELLER
SWEDEN
NORWAY
61°
60°
10°
11°
12°
EAST

Fig. 1

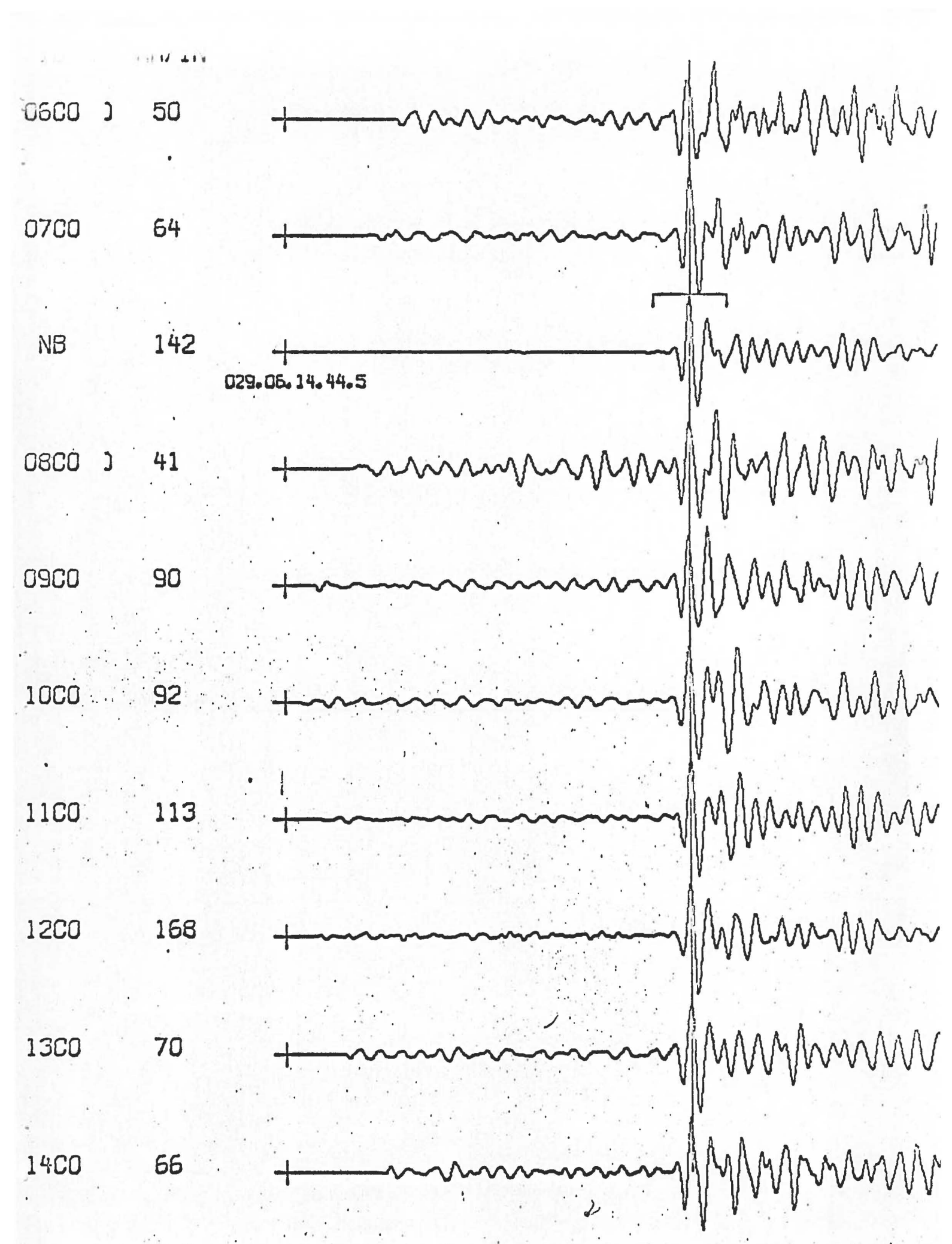
0600) 50
0700 64
NB 142
029.06.14.44.5
0800) 41
0900 90
1000 92
1100 113
1200 168
1300 70
1400 66

Fig. 2b

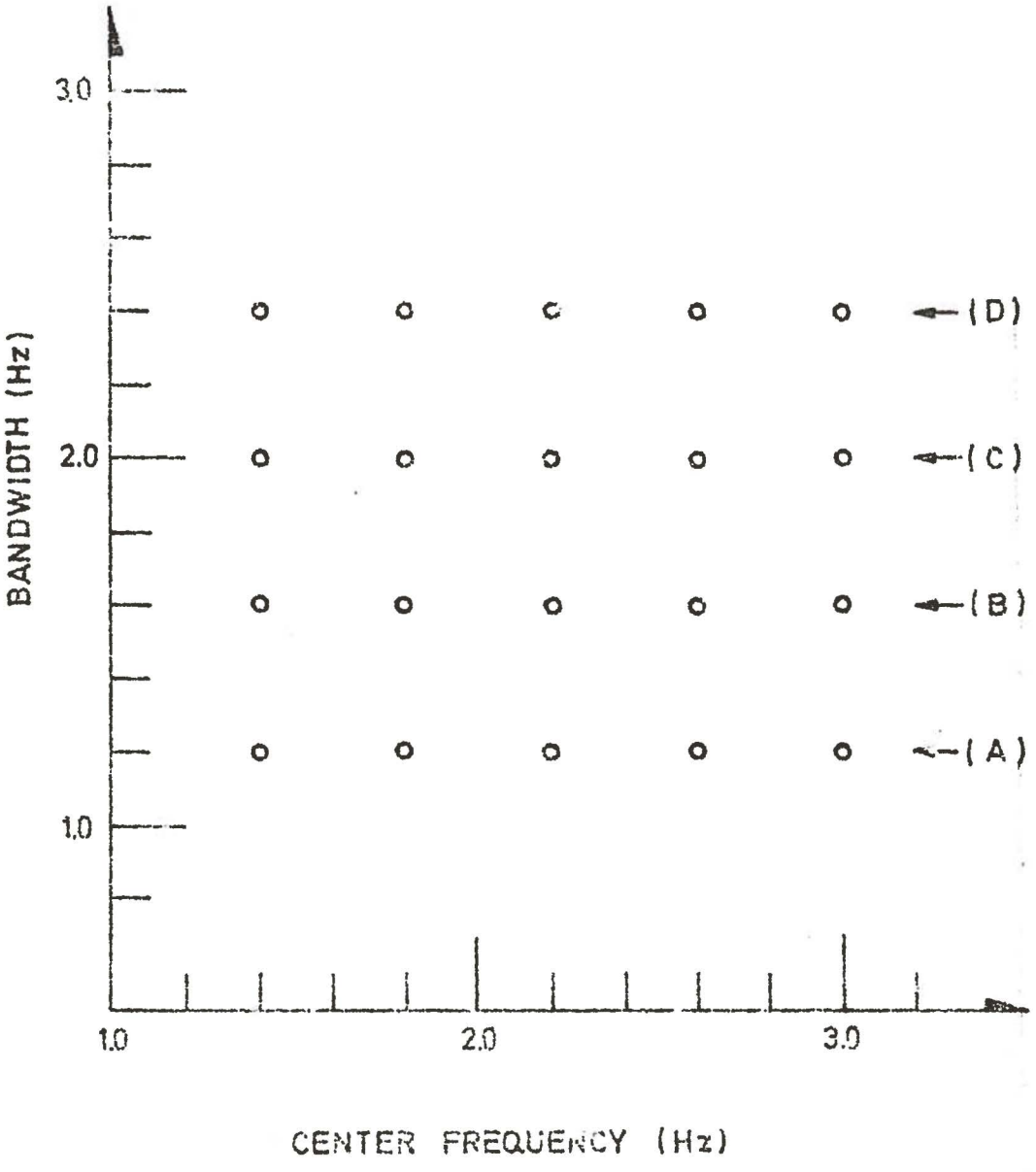

Fig. 3

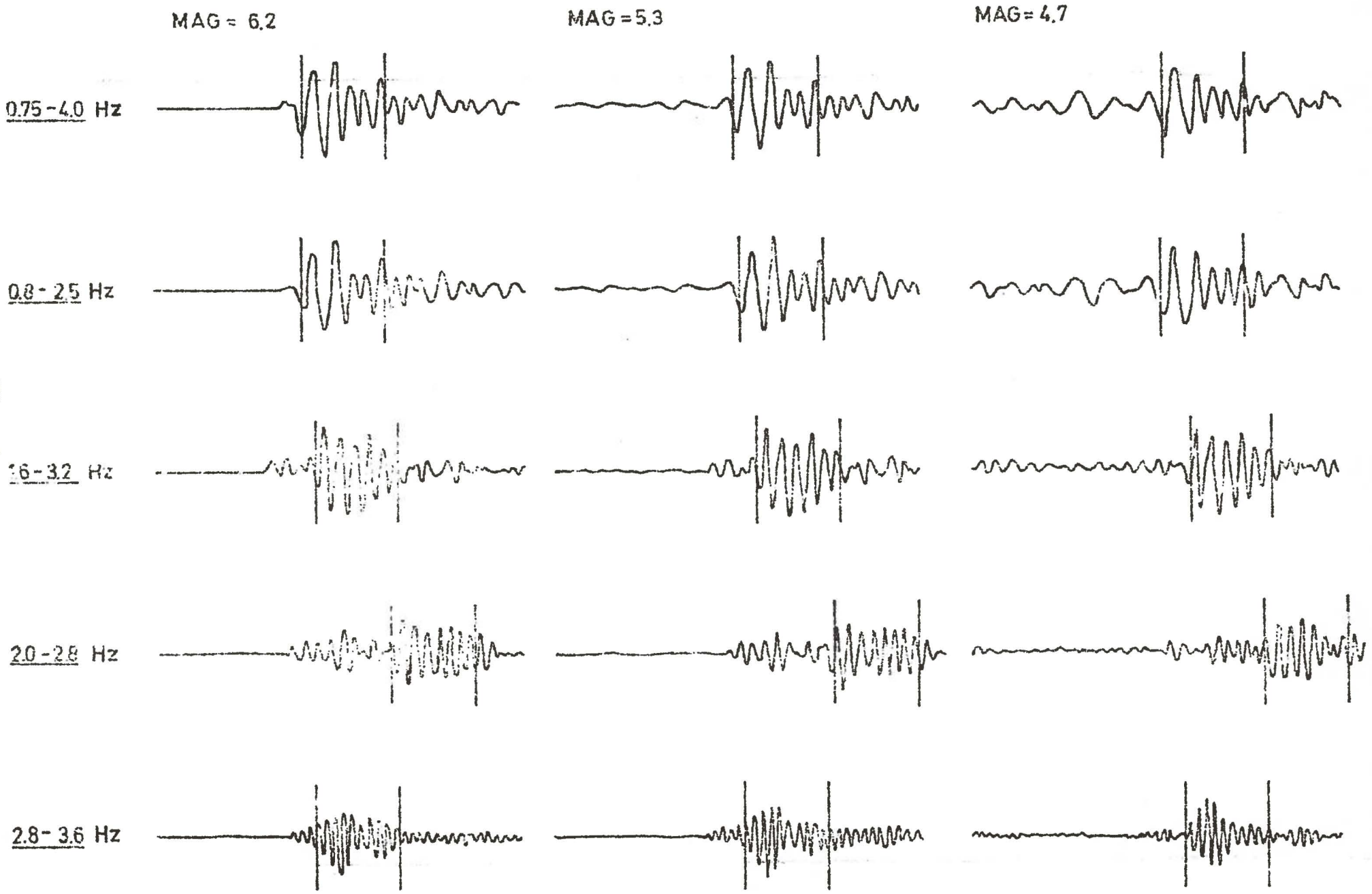

Fig. 4

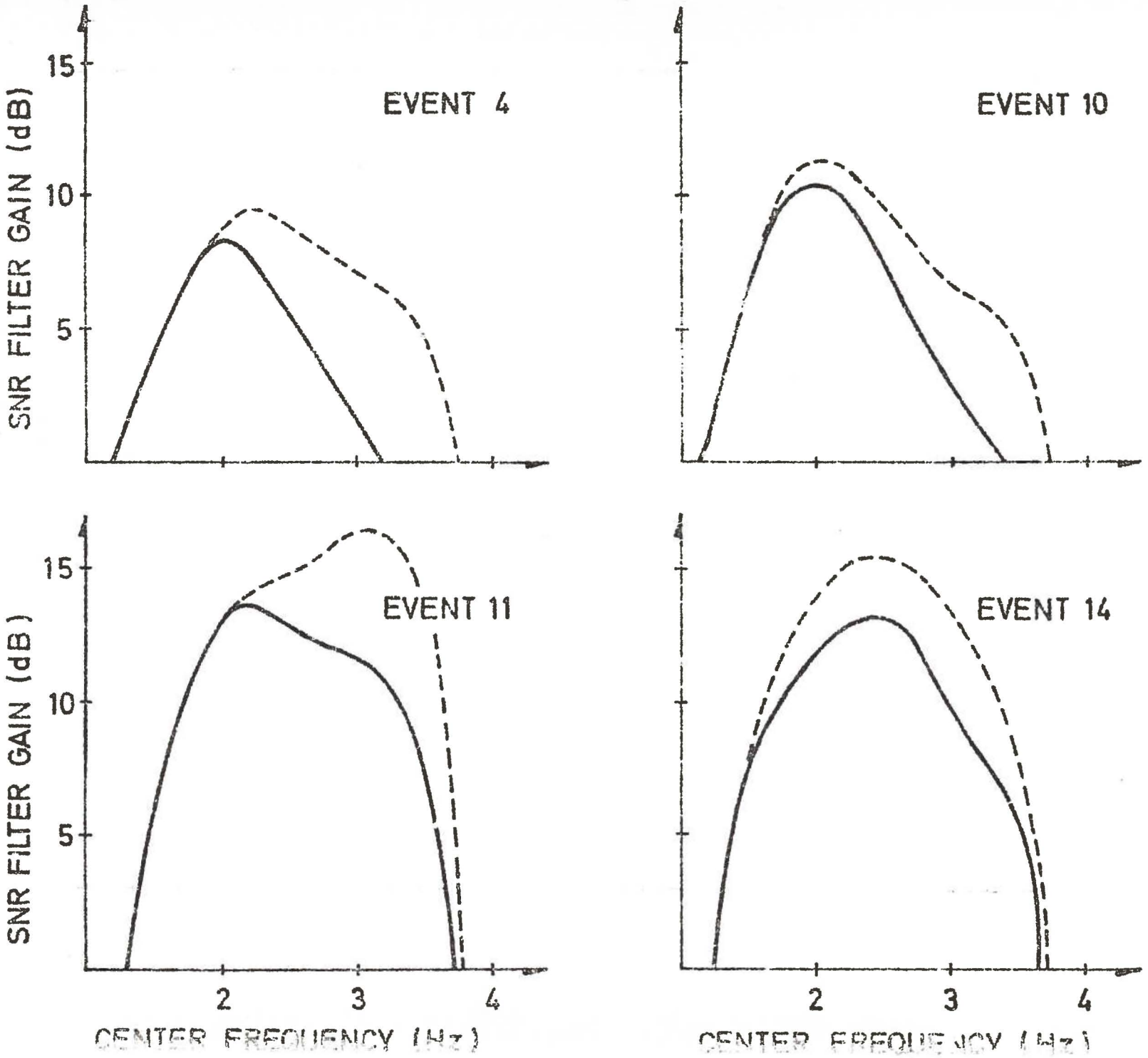
EVENT 4
EVENT 10
EVENT 11
EVENT 14
SNR FILTER GAIN (dB)
SNR FILTER GAIN (dB)
15
10
5
15
10
5
2
3
4
2
3
4
CENTER FREQUENCY (Hz)
CENTER FREQUENCY (Hz)

Fig. 5

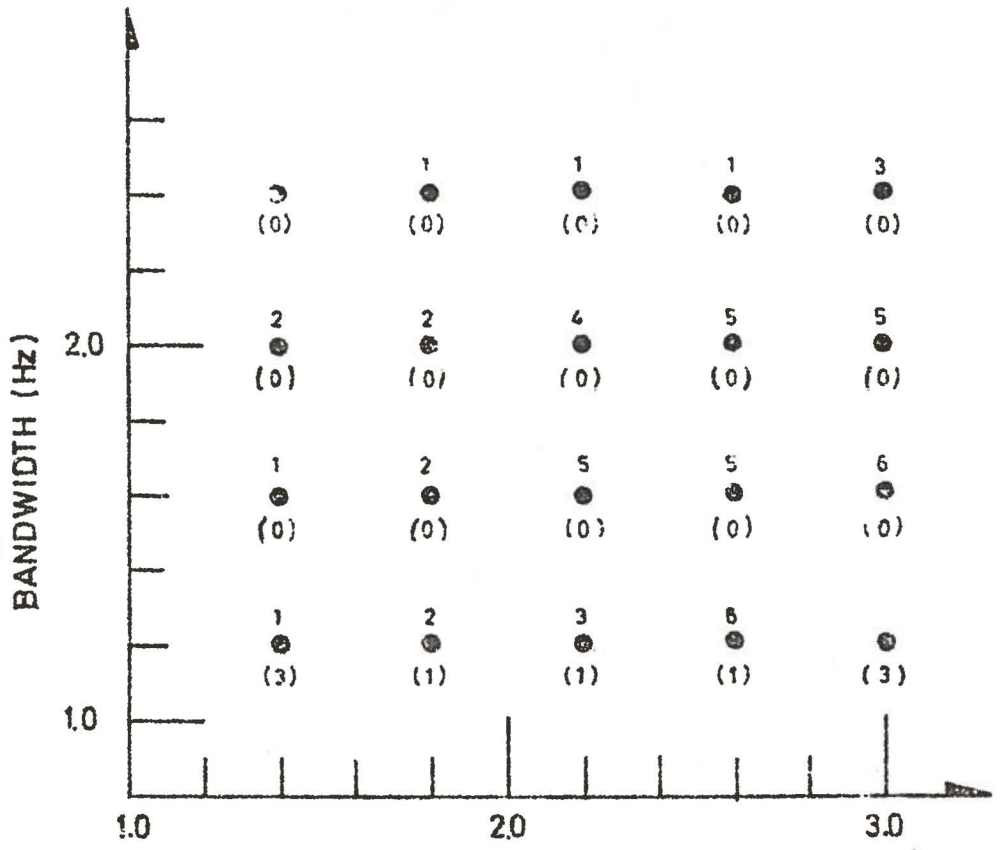
BANDWIDTH (Hz)
2.0
1.0
1.0
2.0
3.0
1 1 1 3
(0) (0) (0) (0) (0)
2 2 4 5 5
(0) (0) (0) (0) (0)
1 2 5 5 6
(0) (0) (0) (0) (0)
1 2 3 6
(3) (1) (1) (1) (3)

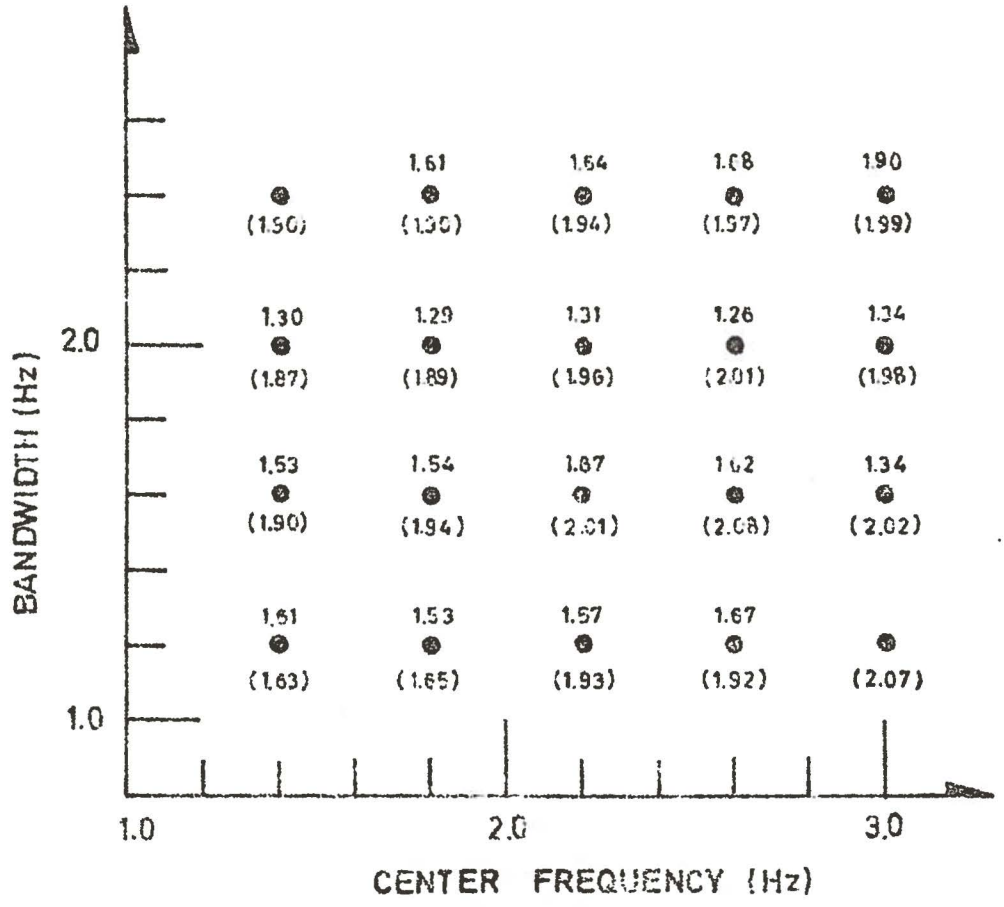
BANDWIDTH (Hz)
2.0
1.0
1.0
2.0
3.0
CENTER FREQUENCY (Hz)
1.61 1.64 1.68 1.90
(1.50) (1.90) (1.94) (1.97) (1.99)
1.30 1.29 1.31 1.26 1.34
(1.87) (1.89) (1.96) (2.01) (1.98)
1.53 1.54 1.87 1.62 1.34
(1.90) (1.94) (2.01) (2.08) (2.02)
1.61 1.53 1.57 1.67
(1.63) (1.65) (1.93) (1.92) (2.07)

Fig. 6 a,b

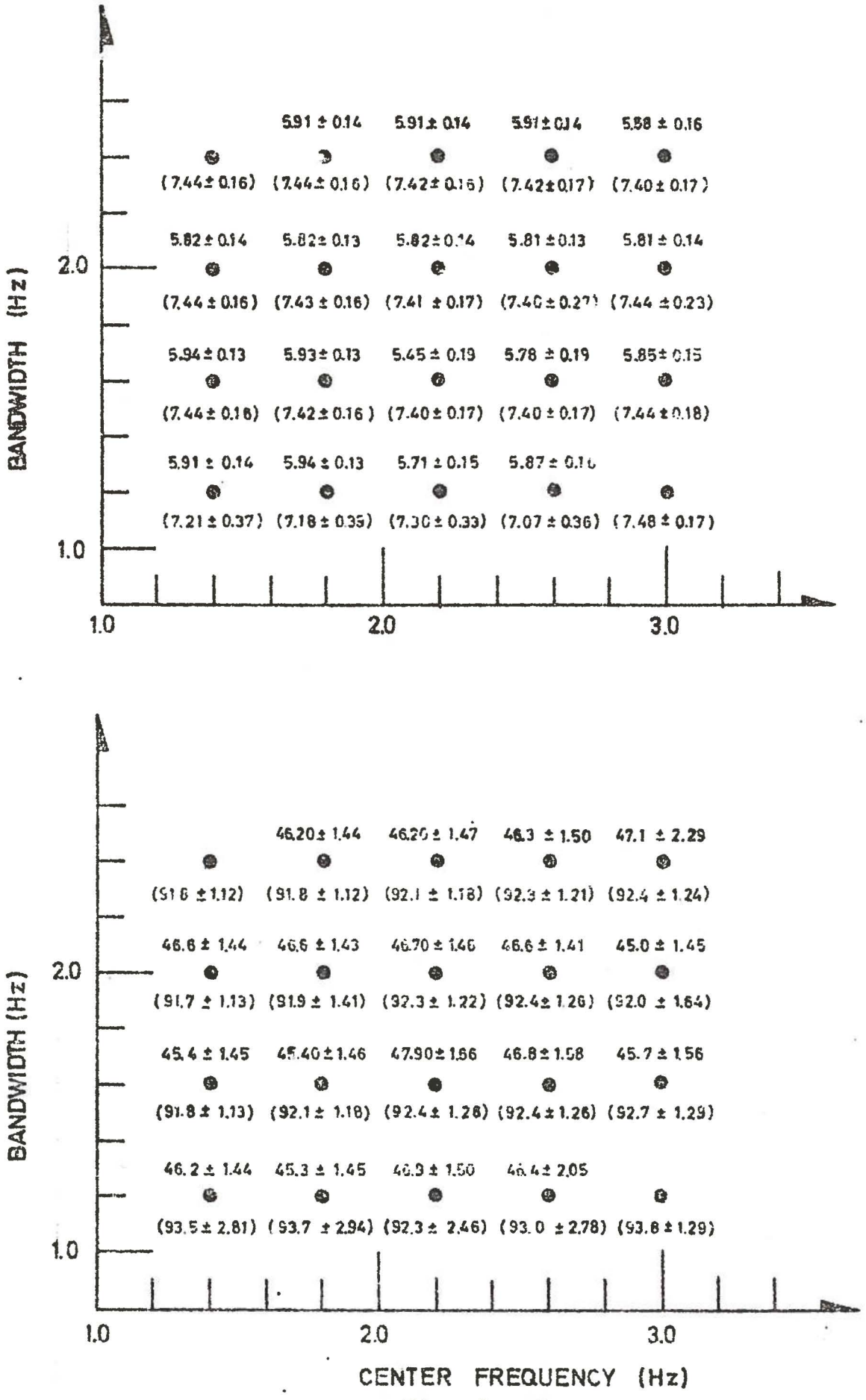
BANDWIDTH (Hz)
2.0
1.0
1.0
2.0
3.0
5.91 ± 0.14
5.91 ± 0.14
5.91 ± 0.14
5.88 ± 0.16
(7.44 ± 0.16)
(7.44 ± 0.16)
(7.42 ± 0.16)
(7.42 ± 0.17)
(7.40 ± 0.17)
5.82 ± 0.14
5.82 ± 0.13
5.82 ± 0.14
5.81 ± 0.13
5.81 ± 0.14
(7.44 ± 0.16)
(7.43 ± 0.16)
(7.41 ± 0.17)
(7.40 ± 0.27)
(7.44 ± 0.23)
5.94 ± 0.13
5.93 ± 0.13
5.45 ± 0.19
5.78 ± 0.19
5.85 ± 0.15
(7.44 ± 0.16)
(7.42 ± 0.16)
(7.40 ± 0.17)
(7.40 ± 0.17)
(7.44 ± 0.18)
5.91 ± 0.14
5.94 ± 0.13
5.71 ± 0.15
5.87 ± 0.16
(7.21 ± 0.37)
(7.18 ± 0.35)
(7.30 ± 0.33)
(7.07 ± 0.36)
(7.48 ± 0.17)
BANDWIDTH (Hz)
2.0
1.0
1.0
2.0
3.0
CENTER FREQUENCY (Hz)
46.20 ± 1.44
46.20 ± 1.47
46.3 ± 1.50
47.1 ± 2.29
(91.8 ± 1.12)
(91.8 ± 1.12)
(92.1 ± 1.18)
(92.3 ± 1.21)
(92.4 ± 1.24)
46.6 ± 1.44
46.6 ± 1.43
46.70 ± 1.46
46.6 ± 1.41
45.0 ± 1.45
(91.7 ± 1.13)
(91.9 ± 1.41)
(92.3 ± 1.22)
(92.4 ± 1.26)
(92.0 ± 1.64)
45.4 ± 1.45
45.40 ± 1.46
47.90 ± 1.66
46.8 ± 1.58
45.7 ± 1.56
(91.8 ± 1.13)
(92.1 ± 1.18)
(92.4 ± 1.26)
(92.4 ± 1.26)
(92.7 ± 1.29)
46.2 ± 1.44
45.3 ± 1.45
46.9 ± 1.50
46.4 ± 2.05
(93.5 ± 2.81)
(93.7 ± 2.94)
(92.3 ± 2.46)
(93.0 ± 2.78)
(93.8 ± 1.29)

Fig. 6 c,d

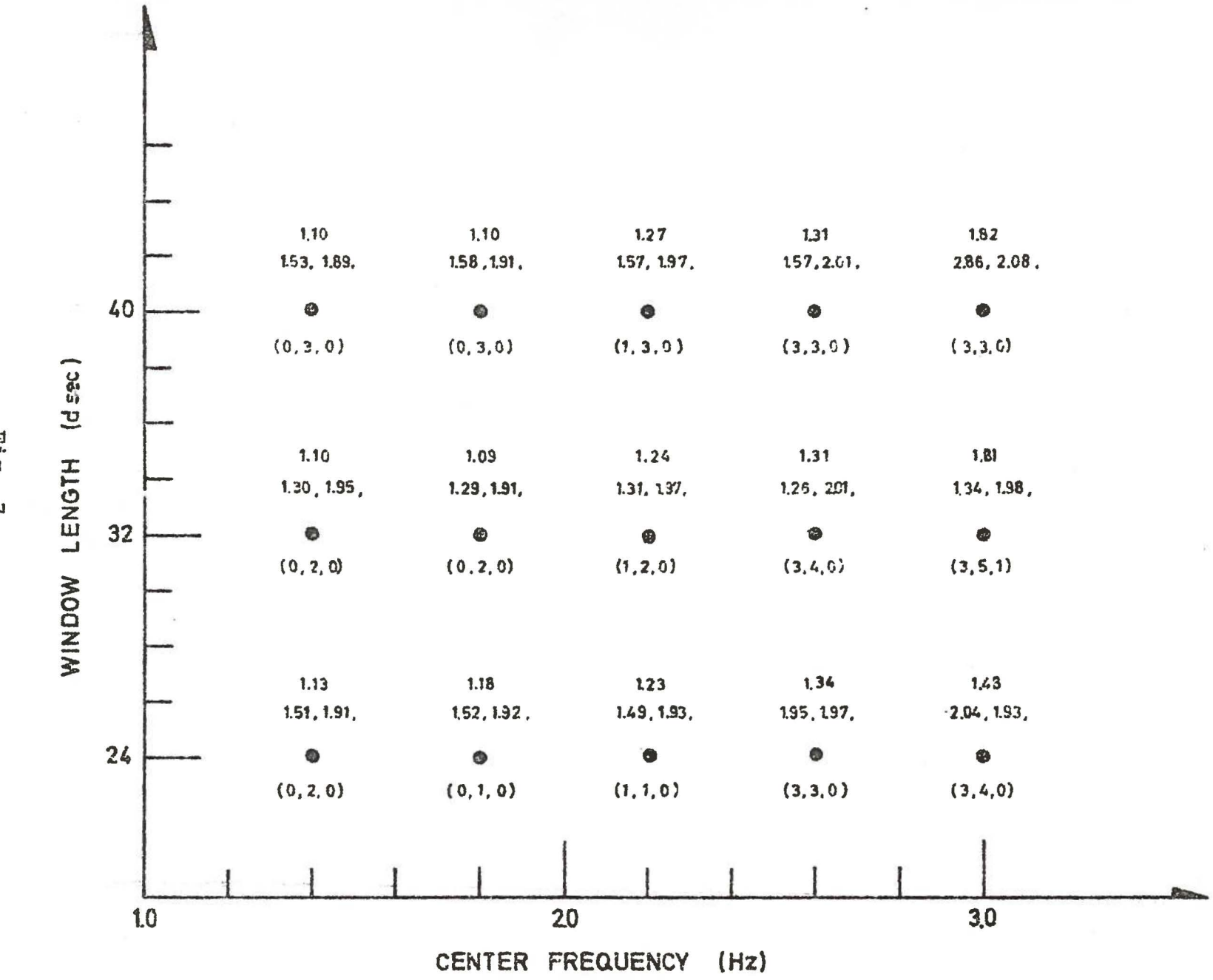
1.10
1.53, 1.89,
(0, 3, 0)
1.10
1.58, 1.91,
(0, 3, 0)
1.27
1.57, 1.97,
(1, 3, 0)
1.31
1.57, 2.01,
(3, 3, 0)
1.82
2.86, 2.08,
(3, 3, 0)
1.10
1.30, 1.95,
(0, 2, 0)
1.09
1.29, 1.91,
(0, 2, 0)
1.24
1.31, 1.97,
(1, 2, 0)
1.31
1.26, 2.01,
(3, 4, 0)
1.81
1.34, 1.98,
(3, 5, 1)
1.13
1.51, 1.91,
(0, 2, 0)
1.18
1.52, 1.92,
(0, 1, 0)
1.23
1.49, 1.93,
(1, 1, 0)
1.34
1.95, 1.97,
(3, 3, 0)
1.43
2.04, 1.93,
(3, 4, 0)
40
32
24
WINDOW LENGTH (d sec)
1.0
2.0
3.0
CENTER FREQUENCY (Hz)

Fig. 7

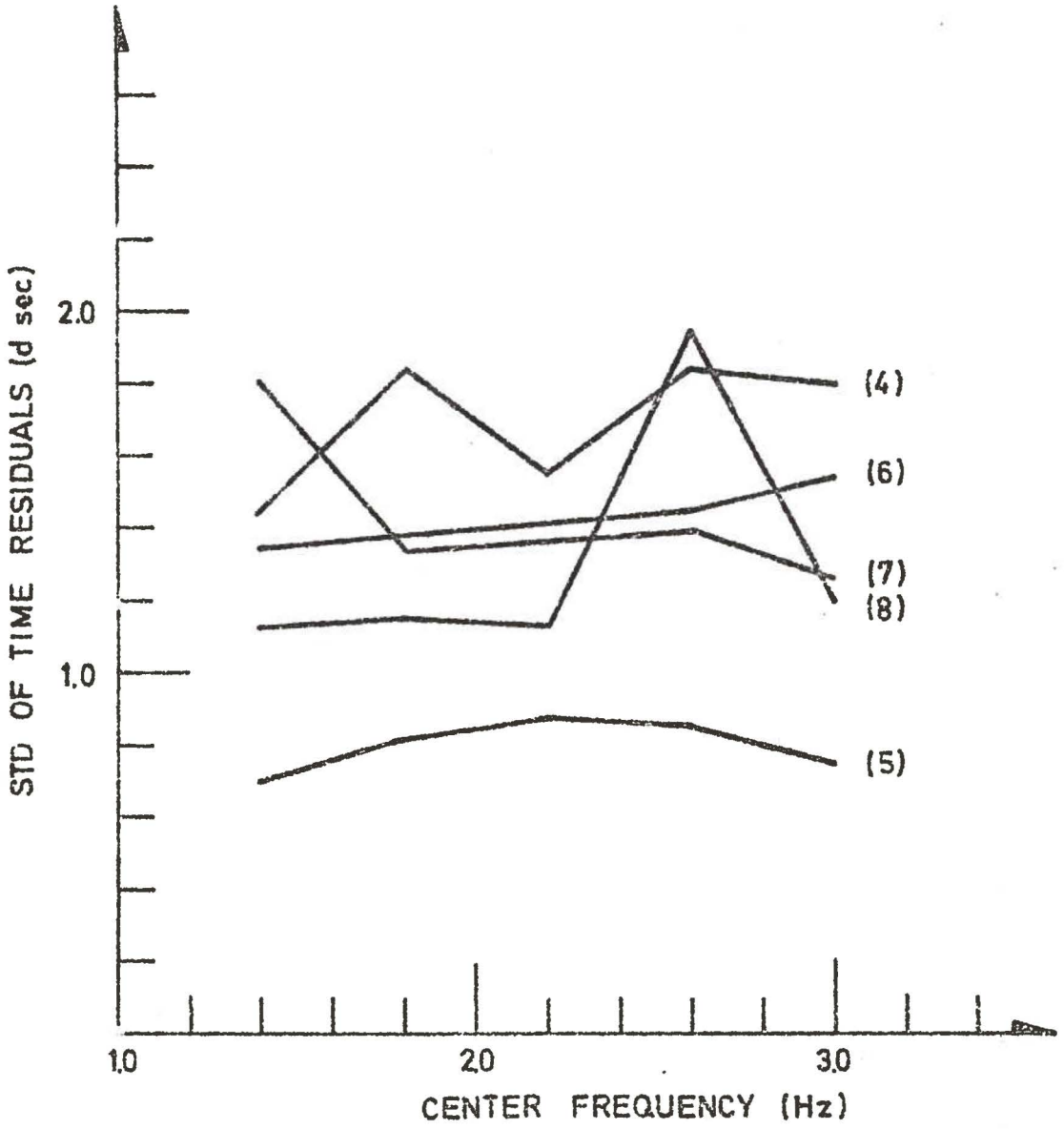
STD OF TIME RESIDUALS (d sec)
2.0
1.0
(4)
(6)
(7)
(8)
(5)
1.0
2.0
3.0
CENTER FREQUENCY (Hz)

Fig. 8